Observation of 1^-0^- Final States from $\psi(2S)$ Decays and e^+e^- Annihilation

N. E. Adam,[1] J. P. Alexander,[1] K. Berkelman,[1] D. G. Cassel,[1] J. E. Duboscq,[1] K. M. Ecklund,[1] R. Ehrlich,[1] L. Fields,[1]
R. S. Galik,[1] L. Gibbons,[1] B. Gittelman,[1] R. Gray,[1] S. W. Gray,[1] D. L. Hartill,[1] B. K. Heltsley,[1] D. Hertz,[1] L. Hsu,[1]
C. D. Jones,[1] J. Kandaswamy,[1] D. L. Kreinick,[1] V. E. Kuznetsov,[1] H. Mahlke-Krüger,[1] T. O. Meyer,[1] P. U. E. Onyisi,[1]
J. R. Patterson,[1] D. Peterson,[1] J. Pivarski,[1] D. Riley,[1] J. L. Rosner,[1,*] A. Ryd,[1] A. J. Sadoff,[1] H. Schwarthoff,[1]
M. R. Shepherd,[1] W. M. Sun,[1] J. G. Thayer,[1] D. Urner,[1] T. Wilksen,[1] M. Weinberger,[1] S. B. Athar,[2] P. Avery,[2]
L. Breva-Newell,[2] R. Patel,[2] V. Potlia,[2] H. Stoeck,[2] J. Yelton,[2] P. Rubin,[3] C. Cawlfield,[4] B. I. Eisenstein,[4] G. D. Gollin,[4]
I. Karliner,[4] D. Kim,[4] N. Lowrey,[4] P. Naik,[4] C. Sedlack,[4] M. Selen,[4] J. J. Thaler,[4] J. Williams,[4] J. Wiss,[4] K. W. Edwards,[5]
D. Besson,[6] K. Y. Gao,[7] D. T. Gong,[7] Y. Kubota,[7] S. Z. Li,[7] R. Poling,[7] A. W. Scott,[7] A. Smith,[7] C. J. Stepaniak,[7]
Z. Metreveli,[8] K. K. Seth,[8] A. Tomaradze,[8] P. Zweber,[8] J. Ernst,[9] A. H. Mahmood,[9] H. Severini,[10] D. M. Asner,[11]
S. A. Dytman,[11] S. Mehrabyan,[11] J. A. Mueller,[11] V. Savinov,[11] Z. Li,[12] A. Lopez,[12] H. Mendez,[12] J. Ramirez,[12]
G. S. Huang,[13] D. H. Miller,[13] V. Pavlunin,[13] B. Sanghi,[13] E. I. Shibata,[13] I. P. J. Shipsey,[13] G. S. Adams,[14] M. Chasse,[14]
J. P. Cummings,[14] I. Danko,[14] J. Napolitano,[14] D. Cronin-Hennessy,[15] C. S. Park,[15] W. Park,[15] J. B. Thayer,[15]
E. H. Thorndike,[15] T. E. Coan,[16] Y. S. Gao,[16] F. Liu,[16] M. Artuso,[17] C. Boulahouache,[17] S. Blusk,[17] J. Butt,[17]
E. Dambasuren,[17] O. Dorjkhaidav,[17] N. Menaa,[17] R. Mountain,[17] H. Muramatsu,[17] R. Nandakumar,[17] R. Redjimi,[17]
R. Sia,[17] T. Skwarnicki,[17] S. Stone,[17] J. C. Wang,[17] K. Zhang,[17] S. E. Csorna,[18] G. Bonvicini,[19] D. Cinabro,[19]
M. Dubrovin,[19] R. A. Briere,[20] G. P. Chen,[20] T. Ferguson,[20] G. Tatishvili,[20] H. Vogel,[20] and M. E. Watkins[20]

(CLEO Collaboration)

[1]*Cornell University, Ithaca, New York 14853, USA*
[2]*University of Florida, Gainesville, Florida 32611, USA*
[3]*George Mason University, Fairfax, Virginia 22030, USA*
[4]*University of Illinois, Urbana-Champaign, Illinois 61801, USA*
[5]*Carleton University, Ottawa, Ontario, Canada K1S 5B6*
and the Institute of Particle Physics, Canada
[6]*University of Kansas, Lawrence, Kansas 66045, USA*
[7]*University of Minnesota, Minneapolis, Minnesota 55455, USA*
[8]*Northwestern University, Evanston, Illinois 60208, USA*
[9]*State University of New York at Albany, Albany, New York 12222, USA*
[10]*University of Oklahoma, Norman, Oklahoma 73019, USA*
[11]*University of Pittsburgh, Pittsburgh, Pennsylvania 15260, USA*
[12]*University of Puerto Rico, Mayaguez, Puerto Rico 00681*
[13]*Purdue University, West Lafayette, Indiana 47907, USA*
[14]*Rensselaer Polytechnic Institute, Troy, New York 12180, USA*
[15]*University of Rochester, Rochester, New York 14627, USA*
[16]*Southern Methodist University, Dallas, Texas 75275, USA*
[17]*Syracuse University, Syracuse, New York 13244, USA*
[18]*Vanderbilt University, Nashville, Tennessee 37235, USA*
[19]*Wayne State University, Detroit, Michigan 48202, USA*
[20]*Carnegie Mellon University, Pittsburgh, Pennsylvania 15213, USA*

Using CLEO data collected from CESR e^+e^- collisions at the $\psi(2S)$ resonance and nearby continuum at $\sqrt{s} = 3.67$ GeV, we report the first significantly nonzero measurements of light vector-pseudoscalar hadron pair production (including $\rho\pi$, $\omega\pi$, $\rho\eta$, and $K^{*0}\bar{K}^0$) and the $\pi^+\pi^-\pi^0$ final state, both from $\psi(2S)$ decays and direct e^+e^- annihilation.

The $\rho\pi$ puzzle poses one of the most enduring questions in strong interaction physics: why is the branching fraction for $\psi(2S) \to \rho\pi$ at least 20 [1] times smaller than expected from scaling the $J/\psi \to \rho\pi$ rate by the ratio of dilepton branching fractions? The "12% rule," a scaling conjecture

generalizing this question for any decay mode, has as its underlying assumption that since charmonium decay to light hadrons must proceed through annihilation of the constituent $c\bar{c}$ into a photon or three gluons, the decay width should be proportional to the square of the $c\bar{c}$ wave

function overlap at the origin. The rule's figure of merit is

$$Q_X = \frac{\mathcal{B}[\psi(2S) \to X]/\mathcal{B}(J/\psi \to X)}{\mathcal{B}[\psi(2S) \to \ell^+\ell^-]/\mathcal{B}(J/\psi \to \ell^+\ell^-)}, \quad (1)$$

where $\mathcal{B}$ denotes a branching fraction and X a particular final state. Decays to dileptons also proceed via $c\bar{c}$ annihilation, and their branching fractions are well measured [1], so their ratio makes a suitable denominator in Eq. (1). Several channels have $Q_X \approx 1$ [1], although some deviations from unity are expected [2]. The $\rho\pi$ mode is not alone: significant suppressions also exist for at least one other vector-pseudoscalar (VP) channel [$K^*(892)^+K^-$] and three vector-tensor channels [$\rho a_2(1320)$, $K^*(892)\bar{K}_2^*(1430)$, and $\omega f_2(1270)$] [1,3].

The continuing struggle to understand the pattern of Q values has provoked many theoretical explanations. For isospin-violating (IV) modes such as $\omega\pi$ and $\rho\eta$, three-gluon mediated decay is suppressed, allowing the electromagnetic process of annihilation into a virtual photon to dominate. Whether $Q_{IV} \sim 1$ remains a crucial open question. A recent review [2] of relevant theory and experiment concludes that none of the proffered theoretical explanations is satisfactory and also finds the underpinnings of the 12% rule overly simplistic.

A major impediment to addressing the puzzle in a systematic manner is the dearth of $\psi(2S)$ branching fraction measurements. Experimental progress on key VP final states has remained dormant for many years. Continuum production, $e^+e^- \to \gamma^* \to X$, which is of interest in its own right [4,5], is expected at levels that may affect $\psi(2S)$ backgrounds and will interfere [6] with $\psi(2S)$ decay, but has not yet been measured. Using e^+e^- collision data acquired with the CLEO detector operating at the Cornell Electron Storage Ring (CESR), this Letter presents $\psi(2S)$ branching fractions and continuum cross sections for $\pi^+\pi^-\pi^0$; $\rho\pi$, $\omega\pi$, $\phi\pi$, $\rho\eta$, $\omega\eta$, $\phi\eta$, $K^{*0}(892)\bar{K}^0$, $K^{*+}(892)K^-$; $b_1(1235)\pi$. Where applicable, the inclusion of charge conjugate states is implied. We use $\rho \to \pi\pi$, $\pi^0 \to \gamma\gamma$, $\omega \to \pi^+\pi^-\pi^0$, $\phi \to K^+K^-$, $\eta \to \gamma\gamma$ and $\pi^+\pi^-\pi^0$, $K^{*0} \to K^-\pi^+$, $K^{*+} \to K_S^0\pi^+$ and $K^+\pi^0$, and $K_S^0 \to \pi^+\pi^-$.

The CLEO III detector [7] features a solid angle coverage of 93% for charged and neutral particles. For the data presented here, the charged particle tracking system operates in a 1.0 T magnetic field along the beam axis and achieves a momentum resolution of ~0.6% at $p = 1$ GeV/c. The cesium iodide (CsI) calorimeter attains photon energy resolutions of 2.2% at $E_\gamma = 1$ GeV and 5% at 100 MeV. Two particle identification systems, one based on ionization energy loss (dE/dx) in the drift chamber and the other a ring-imaging Cherenkov (RICH) detector, are used together to separate $K^\pm$ from $\pi^\pm$. The combined dE/dx-RICH particle identification has efficiencies >90% and misidentification rates <5% for both $\pi^\pm$ and $K^\pm$.

Half of the $\psi(2S)$ data and all the $\sqrt{s} = 3.67$ GeV data were taken after a transition to CLEO-c [8], in which CLEO III's silicon-strip vertex detector was replaced with a six-layer all-stereo drift chamber. The two detector configurations correspond to different accelerator lattices: the former with a single wiggler magnet and a center-of-mass energy spread $\Delta E = 1.5$ MeV, the latter (CESR-c [8]) with the first half of its full complement (12) of wiggler magnets and $\Delta E = 2.3$ MeV.

The integrated luminosity ($\mathcal{L}$) of the data sets was measured using $e^+e^- \to \gamma\gamma$ events [9]. Event counts were normalized with a Monte Carlo (MC) simulation based on the Babayaga [10] event generator combined with GEANT-based [11] detector modeling. The data sets have $\mathcal{L} = 5.63$ pb^{-1} on the peak of the $\psi(2S)$ (2.74 pb^{-1} for CLEO III, 2.89 pb^{-1} for CLEO-c) and 20.46 pb^{-1} at $\sqrt{s} = 3.67$ GeV (all CLEO-c). The scale factor applicable to continuum yields in order to normalize them to $\psi(2S)$ data, $f = 0.268 \pm 0.004$, includes a 2.6% correction to the $\mathcal{L}$ ratio to scale it by $1/s^3$ [5]; the error includes both the relative luminosity and form factor s-dependence uncertainties. We also correct each final state's f for small efficiency differences between the $\psi(2S)$ and continuum samples caused by detector configuration.

We base our event selection on charged particles reconstructed in the tracking system and photon candidates in the CsI calorimeter. Energy and momentum conservation is required of the reconstructed hadrons, which have momenta p_i and total energy E_{vis}. We demand $0.98 < E_{vis}/\sqrt{s} < 1.015$ and $||p_1| - |p_2||/(\sqrt{s}/c) < 0.02$ (for $\pi^+\pi^-\pi^0$, $p_1 = p_{\pi^0}$, and $p_2 = p_{\pi^+} + p_{\pi^-}$), which together suppress backgrounds with missing energy or incorrect mass assignments. The experimental resolutions are smaller than 1% in scaled energy and 2% in scaled momentum difference. In order to suppress hadronic transitions to J/ψ, we reject events in which any of the following fall within 3.05–3.15 GeV: the invariant mass of the two highest momentum tracks; or the recoil mass from the lowest momentum single π^0, $\pi^0\pi^0$ pair, or $\pi^+\pi^-$ pair. Feeddown from $\pi^0\pi^0 J/\psi$, $J/\psi \to \mu^+\mu^-$ into $\pi^+\pi^-\pi^0$, $\rho^+\pi^-$, or $(K^+\pi^0)K^-$ is additionally suppressed by requiring $M(\mu^+\mu^-) < 3.05$ GeV for those channels.

MC studies were used to determine invariant mass windows for intermediate particle decay products. To reduce contamination from $\omega f_2(1270)$ [3] and $\omega f_0(600)$ [12] in $b_1\pi$, we exclude $M_{\pi\pi} < 1.5$ GeV. Similarly, $\rho\eta$ candidates with low mass $\eta\pi^\pm$ states are avoided with $M(\eta\pi^\pm)_{min} > 1.4$ GeV. For $\pi^0 \to \gamma\gamma$, $\eta \to \gamma\gamma$, and $K_S^0 \to \pi^+\pi^-$ candidates we use kinematically constrained fits of the decay products to the parent masses. Fake π^0 and η mesons are suppressed with lateral shower profile restrictions and by requiring that their decays to $\gamma\gamma$ not be too asymmetric.

For $\pi^+\pi^-\pi^0$, $\rho^+\pi^-$, and $\rho\eta$ ($\phi\eta$) with $\eta \to \gamma\gamma$, one of the two final state charged particles must be positively

identified as a $\pi^\pm$ ($K^\pm$), but neither can be positively identified as a $K^\pm$ ($\pi^\pm$). Charged kaons in K^*K must be identified as such, and any $\pi^\pm$ candidate must not be identified as $K^\pm$. Charged particles must not be identified as electrons using criteria based on momentum, calorimeter energy deposition, and dE/dx. The softer charged particle in two-track modes must have $p < 0.425 \times \sqrt{s}/c$ to suppress potential background from $\mu^+\mu^-\gamma$ in which a fake π^0 is found. Both tracks in two-track modes must satisfy $|\cos\theta| < 0.83$, where θ is the polar angle with respect to the e^+ direction.

The efficiency ϵ for each final state is the average obtained from MC simulations [11] of both detector configurations. The VP modes are generated [13,14] with angular distribution $(1 + \cos^2\theta)$ [5], $b_1\pi$ flat in $\cos\theta$, and $\pi^+\pi^-\pi^0$ as in ω decay. We assume $\mathcal{B}(b_1 \to \omega\pi) = 100\%$.

Background contamination from other $\psi(2S)$ decays is determined from sidebands neighboring the signal windows in π^0, η, ω, ϕ, K_S^0, K^*, and b_1 candidate mass distributions. The sideband yields from the $\psi(2S)$ sample are decremented by the corresponding number of scaled continuum events (because scaled continuum events inside the signal window are subtracted separately) and by the small residual signal contributions expected and then scaled to match the signal window size.
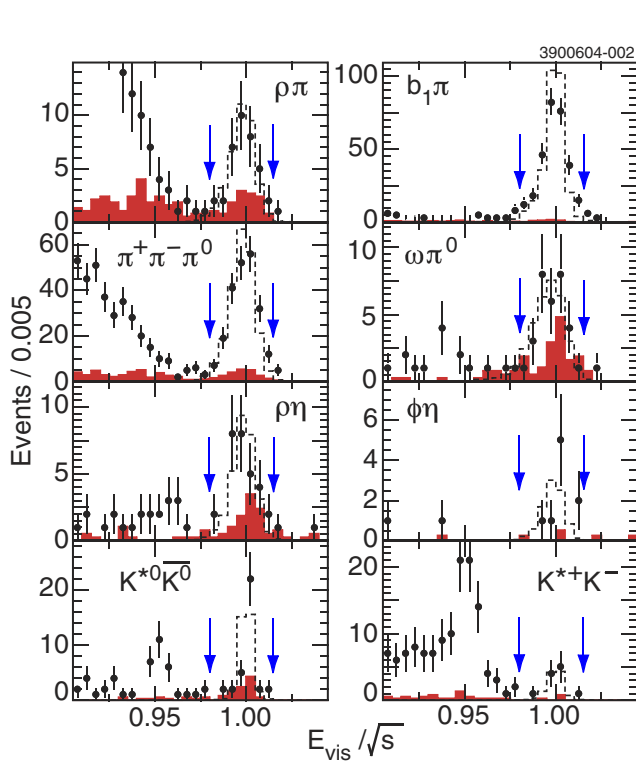
We normalize the branching fractions to the total number of produced $\psi(2S)$ events. The technique described in Ref. [15] is applied to the data sets used here, resulting in a total number of $\psi(2S)$ decays of 3.08×10^6.

Kinematic distributions are shown in Figs. 1–4 and the event totals and efficiencies in Table I. We observe signals for several modes in both $\psi(2S)$ and continuum data sets. The significances S in the last column of Table I reflect the likelihood that the $\psi(2S)$ yields cannot be attributed to backgrounds alone. S is computed from trials in which Poisson fluctuations of the $\psi(2S)$, continuum, and cross-feed contributions are all simulated to obtain a confidence level (C.L.) that a given mean $\psi(2S)$ signal μ combined with backgrounds would exceed or equal the observed event count. S is obtained from this procedure with $\mu = 0$.

Table II shows the final results. We compute branching fractions with a straightforward subtraction of luminosity-scaled continuum yields; the value of the true branching fraction depends on the unknown three-gluon decay amplitudes and corresponding unknown phases. Statistical errors shown correspond to 68% C.L. and upper limits to 90% C.L., and are obtained through simulated trials as described above. Values of Q are computed for each mode based on branching fractions from Ref. [1], except

FIG. 1 (color online). Distributions of scaled visible energy, $E_{\mathrm{vis}}/\sqrt{s}$, for labeled final states. Plots for $\rho\pi$ and $b_1\pi$ sum over the charged and neutral states. Histogram entries are shown for $\psi(2S)$ data (points with error bars), scaled continuum (shaded histogram), and MC (dashed line) with arbitrary normalization. The vertical arrows mark ends of signal selection ranges.
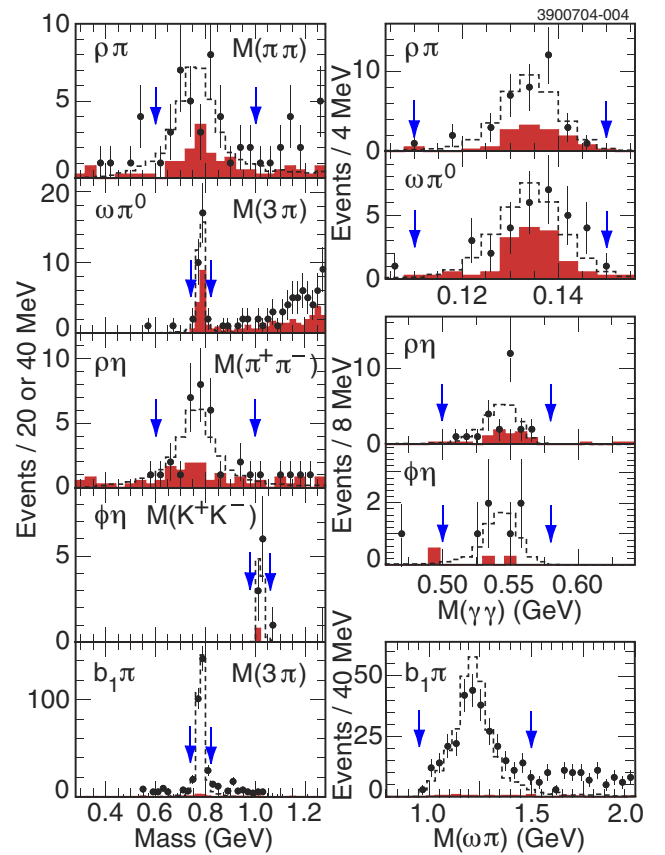

FIG. 2 (color online). Invariant mass distributions relevant to the final states indicated, one entry per event. Symbols are defined in Fig. 1.
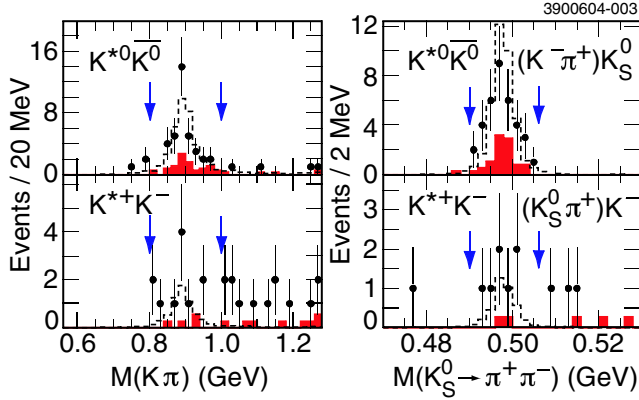
FIG. 3 (color online). Invariant masses for the $K^*(892)$ (left) and K_S^0 (right) candidates, one entry per event, for the final states indicated. Symbols are defined in Fig. 1.

for $\mathcal{B}(J/\psi \to \pi^+\pi^-\pi^0) = (2.10 \pm 0.12)\%$ [16]. Born-level cross sections at $\sqrt{s} = 3.67$ GeV are also given and include an upward adjustment of 20% to account for initial state radiation [10].

The systematic errors on branching fractions share common contributions from the number of produced $\psi(2S)$ events (3%), uncertainty in f (1.5%), trigger efficiency (1%), electron veto (0.5% per veto), and MC statistics (2%). Other sources of uncertainty vary by channel; listed
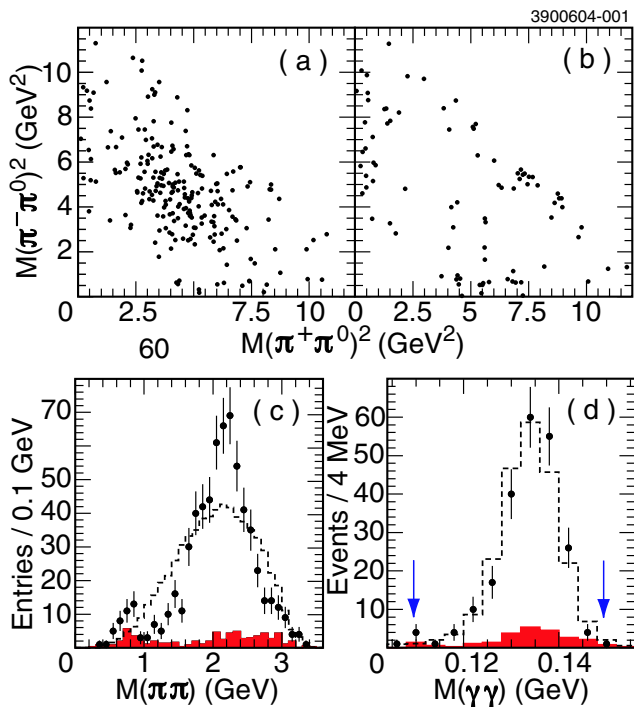

FIG. 4 (color online). Distributions for the $\pi^+\pi^-\pi^0$ final state: the Dalitz plots for (a) $\psi(2S)$ and (b) continuum data; (c) the $\pi^+\pi^-$, $\pi^+\pi^0$, and $\pi^-\pi^0$ mass combinations (3 entries/event), and (d) the $\gamma\gamma$ mass. Symbols are defined in Fig. 1.

TABLE I. For each mode: the efficiency, ϵ; for $\sqrt{s} = 3.67$ GeV data, the number of events, N_c, and background from sidebands, N_{cb}; for $\psi(2S)$ data, the number of events, N_{2S}, the estimated continuum background, fN_c, and background from other $\psi(2S)$ decays, N_b; and the statistical significance S of the $\psi(2S)$ signal in units of a Gaussian standard deviation.

Mode	$\epsilon(\%)$	N_c	N_{cb}	N_{2S}	fN_c	N_b	S
$\pi^+\pi^-\pi^0$	33.5	85	14	219	23.0	2.3	>6
$\rho\pi$	28.8	47	7	36	12.8	1.6	4.0
$\rho^0\pi^0$	31.0	21	4	15	5.6	0.6	2.7
$\rho^+\pi^-$	27.7	26	3	21	7.1	1.0	3.3
$\omega\pi$	19.1	55	9	31	14.7	1.9	2.9
$\phi\pi$	15.8	3	2	1	0.8	1.5	<1
$\rho\eta$	19.5	38	2	29	10.2	0.9	3.9
$\omega\eta$	10.2	3	0	1	0.8	1.5	<1
$\phi\eta$	9.4	3	0	9	0.8	2.4	2.1
$K^{*0}\bar{K}^0$	8.7	36	2	35	9.7	0.5	5.1
$K^{*+}K^-$	16.7	4	2	11	1.1	3.3	2.2
$b_1\pi$	10.9	22	4	288	5.8	70.0	>6
$b_1^0\pi^0$	6.2	5	2	55	1.3	9.0	>6
$b_1^+\pi^-$	13.2	17	2	233	4.5	58.0	>6

with their contribution to the systematic error, they stem from cross-feed subtractions (the change induced by $\pm 50\%$ cross-feed variation), accuracy of MC-generated polar angle and mass distributions (10% for $b_1\pi$, 14%

TABLE II. For each final state X: the branching fraction $\mathcal{B}[\psi(2S) \to X]$, with statistical (68% C.L.) and systematic errors; the upper limit (90% C.L.), U.L., for $\mathcal{B}$; Q from Eq. (1); and σ, the $e^+e^- \to X$ Born-level cross section at $\sqrt{s} = 3.67$ GeV.

Mode	$\mathcal{B}$ (10^{-6})	U.L. (10^{-6})	Q (10^{-2})	σ (pb)
$\pi^+\pi^-\pi^0$	$188^{+16}_{-15} \pm 28$	239	7.0 ± 1.3	$12.3^{+1.9}_{-1.7} \pm 2.7$
$\rho\pi$	$24^{+8}_{-7} \pm 2$	38	1.5 ± 0.5	$8.0^{+1.7}_{-1.4} \pm 1.1$
$\rho^0\pi^0$	$9^{+5}_{-4} \pm 1$	17	1.7 ± 1.1	$3.1^{+1.1}_{-0.9} \pm 0.5$
$\rho^+\pi^-$	$15^{+7}_{-6} \pm 2$	27	1.4 ± 0.7	$4.9^{+1.4}_{-1.1} \pm 0.7$
$\omega\pi$	$25^{+12}_{-10} \pm 2$	44	46 ± 24	$14.0^{+2.7}_{-2.3} \pm 2.0$
$\phi\pi$	$-$	7	$-$	$0.2^{+1.3}_{-0.2} \pm 0.1$
$\rho\eta$	$30^{+11}_{-9} \pm 2$	48	122 ± 49	$10.6^{+2.2}_{-1.9} \pm 1.7$
$\omega\eta$	$-$	11	<6.1	$1.7^{+1.7}_{-0.9} \pm 0.1$
$\phi\eta$	$20^{+15}_{-11} \pm 4$	49	24 ± 19	$1.9^{+1.9}_{-1.0} \pm 0.2$
$K^{*0}\bar{K}^0$	$92^{+27}_{-22} \pm 9$	141	17 ± 6	$22.4^{+4.7}_{-4.0} \pm 2.7$
$K^{*+}K^-$	$13^{+10}_{-7} \pm 3$	31	2.0 ± 1.6	$0.7^{+1.3}_{-0.6} \pm 0.7$
$b_1\pi$	$642^{+58}_{-56} \pm 135$	874	95 ± 26	$9.4^{+3.2}_{-2.6} \pm 2.2$
$b_1^0\pi^0$	$235^{+47}_{-42} \pm 40$	346	80 ± 30	$2.7^{+3.4}_{-1.9} \pm 2.0$
$b_1^+\pi^-$	$418^{+43}_{-42} \pm 92$	579	109 ± 33	$6.5^{+2.4}_{-1.8} \pm 1.2$

for $\pi^+\pi^-\pi^0$), and imperfect modeling of charged particle tracking (1% per track), π^0, η, and K_S^0 finding (2% per π^0 or η, 5% per K_S^0), $\pi^\pm/K^\pm$ identification (3% per identified π/K), and mass resolutions (2%). Cross section systematic errors include the above contributions, substituting an uncertainty in $\mathcal{L}$ (3%) for the normalization error and accounting for uncertainties in the effects of initial and final state radiation (7%). Except for $b_1\pi$ and $\pi^+\pi^-\pi^0$, statistical errors dominate.

The $\psi(2S)$ results in Table II are consistent with previous measurements [1], where available. Unlike other VP channels, the isospin-violating modes $\omega\pi$ and $\rho\eta$ are not strongly suppressed with respect to the 12% rule, an important new piece of the $\rho\pi$ puzzle. The ratio $\mathcal{B}[\psi(2S) \to K^{*+}K^-]/\mathcal{B}[\psi(2S) \to K^{*0}\bar{K}^0] = 0.14^{+0.08}_{-0.06}$ is found to be much smaller than the equivalent ratio for J/ψ decays, 1.19 ± 0.15 [1]. Figure 4 shows that $\psi(2S) \to \pi^+\pi^-\pi^0$ decays have not only a distinct $\rho\pi$ component above the continuum contribution, but, unlike $J/\psi \to \pi^+\pi^-\pi^0$ [16], which is dominated by $\rho\pi$, also feature a much larger cluster of events near the center of the Dalitz plot. The $\rho\pi$ results reported here do not account for any cross feed from this non-$\rho\pi$ component due to its uncertain source and shape. If five events inside the ρ mass window were attributed to the higher mass structure, the $\rho\pi$ branching fraction would decrease by a quarter and its significance by one unit.

The SU(3) expectation [17] for continuum cross sections is $\omega\pi : \rho\eta : K^{*0}\bar{K}^0 : \rho\pi : \phi\eta : K^{*+}K^- : \omega\eta : \phi\pi = 1 : 2/3 : 4/9 : 1/3 : 4/27 : 1/9 : 2/27 : 0$, in which a mixing angle θ_p satisfying $\sin\theta_p = -1/3$, $\cos\theta_p = 2\sqrt{2}/3$ is chosen to describe η-η' mixing. With the striking exception of $K^{*0}\bar{K}^0$, the measured VP continuum cross sections are consistent with Born-level calculations [6,18] and the above ratio predictions from SU(3). A least-squares fit for the common unit of cross section [corresponding to $\sigma(\omega\pi)$], excluding $K^{*0}\bar{K}^0$, yields $\sigma_{\text{fit}} = 16.4 \pm 2.7$ pb with $\chi^2 = 4.9$ for 6 d.o.f.; $\sigma(K^{*0}\bar{K}^0)$ exceeds $(4/9)\sigma_{\text{fit}}$ by 3.0 standard deviations. Variations in θ_p of $\pm 10°$ induce changes of $^{+0.7}_{-1.2}$ pb in σ_{fit}.

In summary, we have presented first evidence for $\psi(2S)$ decays to $\pi^+\pi^-\pi^0$, $\rho\pi$, $\rho\eta$, and $K^{*0}\bar{K}^0$. Measurements for several other VP channels are also given. The results suggest that, for VP final states, $\psi(2S)$ decays through three gluons are severely suppressed with respect to the 12% rule and the corresponding electromagnetic processes are not. The decay $\psi(2S) \to \pi^+\pi^-\pi^0$ exhibits a $\rho \to \pi\pi$ signal but has a much larger component at higher $\pi\pi$ mass. Continuum e^+e^- cross sections for these final states are presented for the first time.

We gratefully acknowledge the effort of the CESR staff in providing us with excellent luminosity and running

*On leave of absence from University of Chicago.
[1] Particle Data Group, S. Eidelman *et al.*, Phys. Lett. B **592**, 1 (2004).
[2] Y. F. Gu and X. H. Li, Phys. Rev. D **63**, 114019 (2001).
[3] BES Collaboration, J. Z. Bai *et al.*, Phys. Rev. D **69**, 072001 (2004).
[4] P. Wang, C. Z. Yuan, and X. H. Mo, Phys. Rev. D **69**, 057502 (2004).
[5] S. J. Brodsky and G. P. Lepage, Phys. Rev. D **24**, 2848 (1981).
[6] P. Wang, C. Z. Yuan, and X. H. Mo, Phys. Lett. B **574**, 41 (2003).
[7] CLEO Collaboration, Y. Kubota *et al.*, Nucl. Instrum. Methods Phys. Res., Sect. A **320**, 66 (1992); D. Peterson *et al.*, Nucl. Instrum. Methods Phys. Res., Sect. A **478**, 142 (2002); M. Artuso *et al.*, Nucl. Instrum. Methods Phys. Res., Sect. A **502**, 91 (2003).
[8] CLEO-c/CESR-c Taskforces and CLEO-c Collaboration, Cornell University LEPP Report No. CLNS 01/1742 (2001) (unpublished).
[9] CLEO Collaboration, G. Crawford *et al.*, Nucl. Instrum. Methods Phys. Res., Sect. A **345**, 429 (1992).
[10] C. M. Carloni Calame *et al.*, in *Proceedings of the Workshop on Hadronic Cross-Section at Low-Energy (SIGHAD03), 8-10 October 2003, Pisa, Italy*, edited by M. Incagli and G. Graziano (Elsevier, Amsterdam, 2004), p. 258.
[11] Computer code GEANT 3.21, in R. Brun *et al.*, CERN Report No. W5013, 1993 (unpublished).
[12] BES Collaboration, M. Ablikim *et al.*, Phys. Lett. B **598**, 149 (2004).
[13] D. J. Lange, Nucl. Instrum. Methods Phys. Res., Sect. A **462**, 152 (2001).
[14] E. Barberio and Z. Was, Comput. Phys. Commun. **79**, 291 (1994).
[15] CLEO Collaboration, S. B. Athar *et al.*, Phys. Rev. D **70**, 112002 (2004).
[16] BES Collaboration, J. Z. Bai *et al.*, Phys. Rev. D **70**, 012005 (2004).
[17] H. E. Haber and J. Perrier, Phys. Rev. D **32**, 2961 (1985); L. Kopke and N. Wermes, Phys. Rep. **174**, 67 (1989).
[18] P. Wang, X. H. Mo, and C. Z. Yuan, Phys. Lett. B **557**, 192 (2003).
[19] BES Collaboration, M. Ablikim *et al.*, hep-ex/0407037; hep-ex/0408047; Phys. Rev. D **70**, 112003 (2004); **70**, 112007 (2004).